NON-THERMAL EMISSION IN ASTROPHYSICAL ENVIRONMENTS: FROM PULSARS TO SUPERNOVA REMNANTS

A Dissertation

Submitted to the Faculty

of

Purdue University

by

David Lomiashvili

In Partial Fulfillment of the

Requirements for the Degree

of

Doctor of Philosophy

May 2013

Purdue University

West Lafayette, Indiana

ProQuest LLC.
789 East Eisenhower Parkway
P.O. Box 1346
Ann Arbor, MI 48106 - 1346

4. Non-Thermal High-Energy Spectra of the Pulsar Wind Nebulae

4.1 Introduction

Pulsars continuously dissipate their rotational energy via the winds of relativistic particles. Confinement of these outflows creates pulsar wind nebulae (PWNe), luminous objects seen across the electromagnetic spectrum. These sources can be used as important probes of relativistic shocks, particle acceleration, and ambient properties.

We will skip a discussion of the details of how the wind is generated and here simply assume that the pulsar's continuous energy injection ultimately results in the wind that generates synchrotron and IC emission.

A pulsar-driven wind decelerates as it expands into the cold, slowly expanding supernova ejecta, producing a termination shock (TS), at which leptons are accelerated to ultrarelativistic energies.

Particles do not radiate upstream of the TS, but flow relativistically along with the frozen-in magnetic field. At the shock, particles are thermalized and reaccelerated, producing synchrotron emission in the downstream flow.

At radio wavelengths the spectra of PWNe are characterized by a flat power-law, with index ($\sim 0 - 0.3$) and a steeper power-law in X rays ($\sim 0.7 - 1$). Usually this spectral steepening is attributed to the aging of the particles (due to radiative cooling); However, in that case the expected increase in spectral index should be ~ 0.5, which is smaller than what is typically observed [96]. Moreover, in some PWNe multiple (more than two) spectral breaks are observed. In addition to particle cooling, they can be produced by a rapid decline in the pulsar output over time [89] or the intrinsic spectrum of the injected particles, which may deviate from a simple power law.

A spatial evolution of the spectra is expected for the frequencies for which the synchrotron lifetime is shorter than the flow time to the edge of the PWN. This effect is indeed observed in the X-ray spectra of *The Crab Nebula*, *3C 58*, and *G21.5.0.9* [92, 95], but the spectra steepen rather uniformly with radius, whereas current models predict more rapid steepening in the outer regions of PWN [87] (hereafter KC84), [90]. Some mixing of electrons of different ages at each radius seems to be required, perhaps due to diffusion processes in the PWN.

The spectrum of some PWNe goes all the way up to the TeV gamma-rays. Among them, *The Crab Nebula* is probably the most famous. TeV emission is well explained as inverse Compton emission, from the relativistic particles in the shocked wind acting as scattering centers for the photons coming from the omnipresent CMB, starlight and Galactic IR background. This photons can also be supplied by the local environment if the photon density in the synchrotron component is high enough.

There have been a number of analytical models that take into account either the spatial dependence [82, 87, 91] or evolution [83, 84, 86] of the PWN properties but not both. In addition, the conventional PWN models neglect diffusion which can play an important role in evolved PWNe at large distances from the pulsar where the bulk flow decelerates significantly. Being computationally intensive, relativistic MHD simulations of PWNe [88, 94] can only model the region in the vicinity of the termination shock and hence are poorly suited for studying large, evolved PWNe, possibly associated with extended γ-ray sources.

We developed a semi-analytical simplified model of a PWN that is spatially-resolved (i.e. wind properties will vary with the distance from the pulsar) and take into account diffusion.

4.2 Model

The morphology of a young PWN is expected to be elongated along the pulsar spin axis due to the higher equatorial pressure associated with the toroidal magnetic

field [82]. This effect is seen clearly in observed images of many PWNe as well as in simulations [88] (e.g., Fig. 4.1 (a)-(b)) and allows one to infer the likely projected orientation of the pulsar. So, the choice of axially symmetric, spherically expanding torus (Fig. 4.1 (c)) as a geometrical model for PWN seems reasonable.

Since the change of the PWN size due to compression by the reverse SNR shock or due to the decreasing pulsar spin-down rate occur on longer time-scales than those associated with the bulk and diffusive particle motion, we will be considering a steady state model. However, it should be noted that, if the synchrotron lifetime of emitting particles is a significant fraction of the PWN age (as is almost always the case at radio wavelengths, and sometimes also in X rays), then the PWN emission represents an integrated history of the pulsar's spin down, and evolution of the nebula should be taken in account.

We have developed a model with following simplifications: a power-law injection spectrum, no hadronic component, CMB only and fixed outer boundary.

Assuming spherical symmetry and stationarity of the problem, the large-scale structure of the flow will be determined by the stationary MHD solutions of KC84 which provide prescriptions for the magnetic field $B(r)$ and downstream bulk flow speed $V(r)$ of the wind.

In this case the problem is treatable analytically if spatial and energy domains being divided into four different zones with drastically different behavior of the distribution function. Two spatial zones (we will call them "Near" and "Far", see Fig. 4.1 (c)) are similar to the ones in KC84 with a corresponding behavior of $V(r)$ and $B(r)$.

The model includes the effects of diffusion, advection and two types of losses, adiabatic and synchrotron. In this work we consider an energy-independent large-scale diffusion coefficient which could be caused by mixing of the particles by the turbulent flows in the pulsar wind. However, calculations can be carried out for Bohm-type energy-dependent diffusion coefficient as well.

In order to obtain the particle distribution function we solve the kinetic equation for "Near" (closer to the TS) and "Far" (further from the TS) zones separately and match the solutions at the boundary (for more details, see appendix A). As an injection spectrum at the TS we take a simple power-law $n_0 \sim E^{-\Gamma}$.

$$-\nabla \left(D(\gamma, z) \nabla N(\gamma, z) \right) + \nabla \left(V(z) N(\gamma, z) \right) + \frac{\partial}{\partial \gamma} \left(b(\gamma, z) N(\gamma, z) \right) = 0 \qquad (4.1)$$

As the boundary conditions we require that distribution function ceases at the infinity, while at the termination shock ($z = z_s$) it matches the injection spectrum.

In the Near zone, where flow speed goes as $V(r) \sim V_0 (r/r_0)^{-2}$ (KC84) adiabatic losses absent, magnetic field increases with distance $B(r) \sim B_0 (r/r_0)$, diffusion coefficient decreases $D(r) \sim D_0 (r/r_0)^{-1}$ and synchrotron loss term: $b_{synch}(r, E) \sim b_{synch}(E)(r/r_0)^2$. Resulted particle number density has a power-law dependence on energy with an exponential cut-off, $n \sim E^{-\Gamma} \exp\left(-E/E^c_{Near}\right)$. Cut-off energy E^c_{Near} depends on the parameters of the model $(V_0, B_0, D_0, r_0, \sigma)$ as well as on the distance from the shock.

In the Far zone plasma flows with a constant speed V_0, magnetic field decays with distance $B(r) \sim B_0 (r/r_0)^{-1}$, diffusion coefficient $D(r) \sim D_0 (r/r_0)$, and loss terms $b_{adi}(r, E) \sim b_{adi}(E)(r/r_0)^{-1}$, $b_{synch}(r, E) \sim b_{synch}(E)(r/r_0)^{-2}$. In order to be able to get analytic solutions for the particle density, we divide the energy range into two. This two zones reflect the fact that the adiabatic losses dominate over the radiative ones at lower energies (typical electron Lorentz factors $\sim 100 - 1000$) and vise versa at higher energies. Which means that for X-ray and TeV emitting electrons radiative losses dominate, while expansion losses are important for the radio and GeV emitting electrons.

As a result, particle spectrum in the low energy range does not change and stays the same throughout the whole nebula, $n \sim E^{-\Gamma} \exp\left(-E/E^c_{Near}\right)$ (see Fig. 4.2). This can be easily understood since energy-independent diffusion and adiabatic losses doesn't change the spectrum. On the other hand, high energy particles obey steeper

spectrum with exponential cut-off, $n \sim E^{-\Gamma-1/2} \exp\left(-E/E^{c}_{Far}\right)$ (see Fig. 4.2). In principle, cut-off energy is different from cut-off in Near zone. However it still depends on the parameters of the model and on the distance from the TS. For the detailed calculations on solving the kinetic equation, see appendix A.

After obtaining the solutions for the distribution function, we calculate the total spectra of PWN, by integrating the specific intensity over the volume of nebula. Resulted flux, as a function of energy, has a distinct double-hump shape owing to two emission mechanisms, synchrotron and IC (Fig. 4.3 (a)-(d)).

4.3 Summary

To summarize, we consider two-zone (Near; Far) model and adopt Kennel and Coroniti [87] (KC84) solutions for the radial dependence of the flow velocity and magnetic field. In order to get the analytical solution for the distribution function in the Far zone we also need to determine the energy ranges for which adiabatic losses dominate over synchrotron (low energy) and vise versa (high energy), since simultaneous consideration of both terms significantly complicates the problem. Such treatment is not necessary in the Near zone, since due to the peculiarity of KC84 solution for the flow velocity, adiabatic loss rate equals to zero.

The overall spectrum depends on the wind parameters as well as on the external environment parameters such as the local radiation density and confining ISM pressure. Therefore, fitting of the model to the multiwavelength spectrum of the PWN, combined with the spatial information about the PWN size and surface brightness distribution, can constrain both the wind and the ambient medium parameters.

The net result of our preliminary work is that both the synchrotron and IC spectral emissivities of the pulsar wind are strongly varying across the PWN so that the volume-integrated spectral emissivity (corresponding to an unresolved source from observational point of view for the high energy telescopes) is significantly different

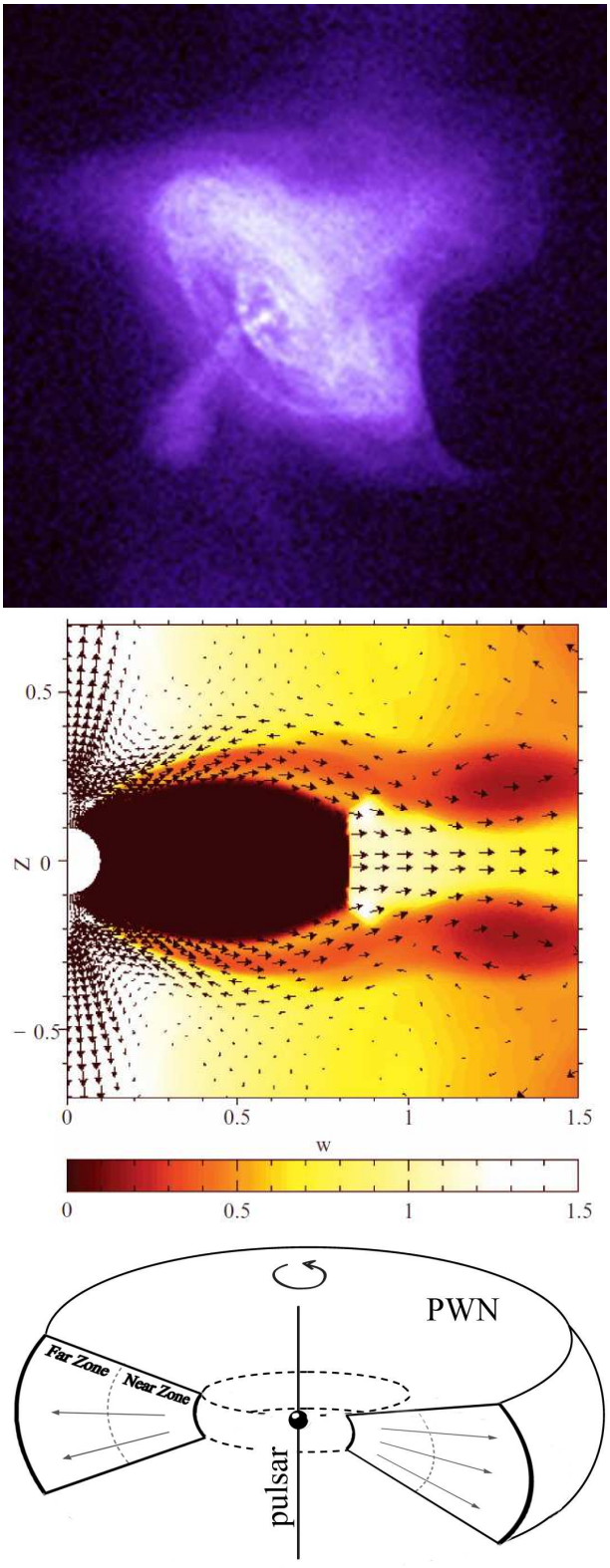

Figure 4.1. Structure of the PWN. (a) X-ray image of Crab; (b) simulated picture of PWN in the equatorial plane; (c) "donut"-type geometry used in our model. Credit: Komissarov and Lyubarsky [88].

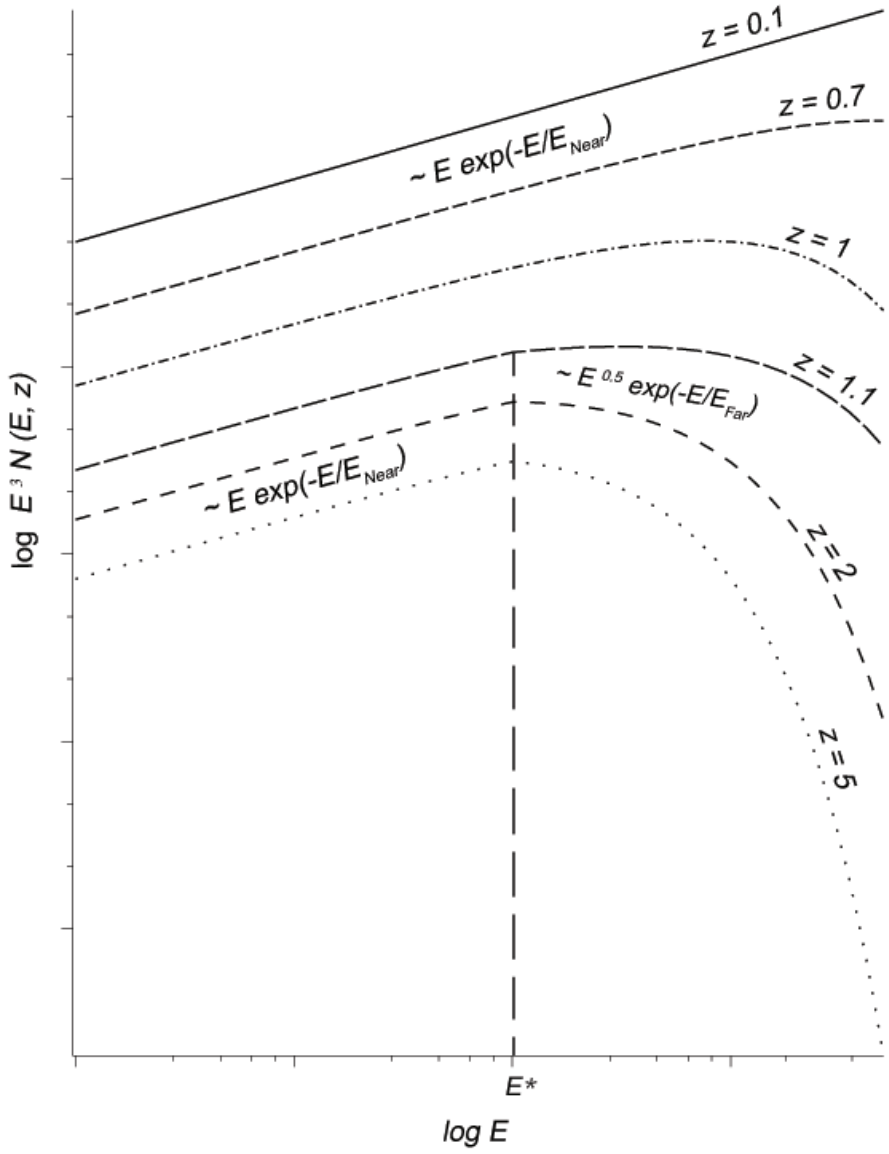

Figure 4.2. Spatially resolved particle spectrum. At the termination shock ($z = 0.1$) particles have a simple power-law distribution which evolves with distance into the power-low with exponential cut-off at E_{Near}. After the flow transition point ($z = 1$), low and high energy particles have different spectra due to the different loss mechanisms. Particles at high energies ($E > E^*$) have steeper spectrum with different cut-off energy (E_{Far}), while low energy ($E < E^*$) particles preserve the same spectrum, since adiabatic losses do not change the spectral dependence. Values of the parameters are $\Gamma = 2; \sigma = 0.003; V_0 r_0/D_0 = 2; B_0 = 3\mu G$. For more clarity each line is normalized arbitrarily.

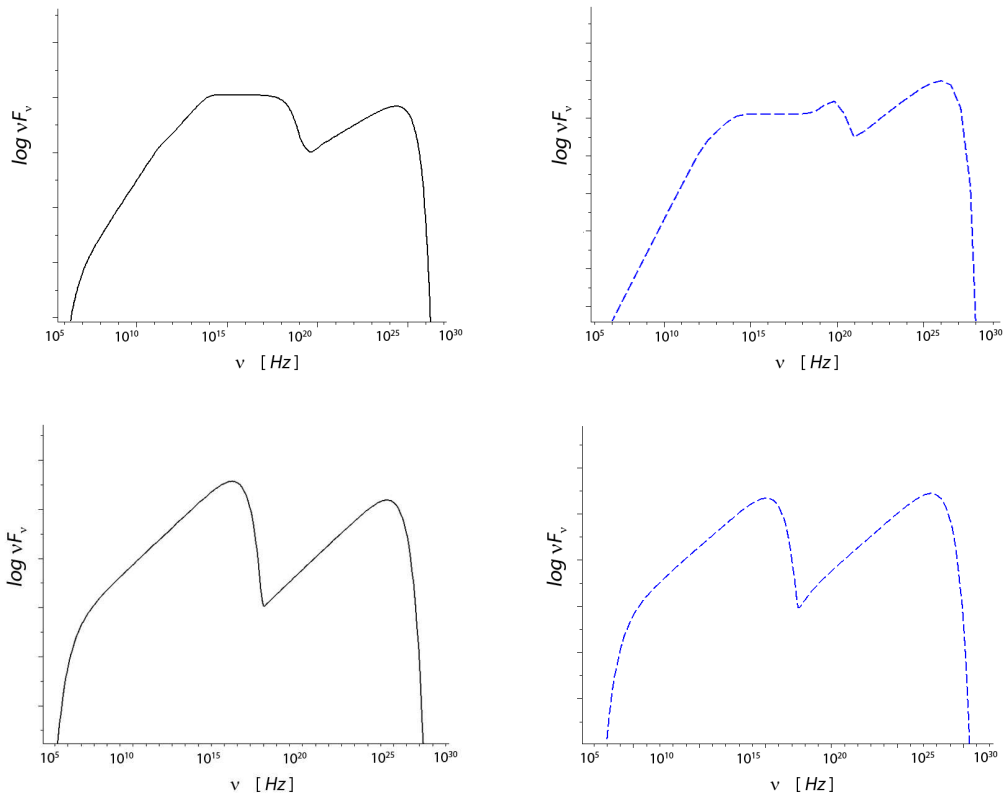

Figure 4.3. Modeled multi-wavelength spectrum of PWN. *Upper row* - Our model, Two-Zone configuration. *Bottom row* - Single-Zone configuration. Values of the parameters are: *solid line*- $\Gamma = 2; \sigma = 0.003; V_0 r_0/D_0 = 0.1; B_0 = 10\mu G; U_{rad} = 2.0 eV/cm^3; z_{PWN} = 50$; *dashed line* - $\Gamma = 2; \sigma = 0.003; V_0 r_0/D_0 = 1; B_0 = 1\mu G; U_{rad} = 0.4 eV/cm^3; z_{PWN} = 50$.

from that obtained in the spatially-uniform (so called "Single-zone") models de Jager et al [84], Fang and Zhang [85], Gelfand et al [86].

Obtained particle distribution function has a cutoff energy which changes with distance from the TS. This in principle could cause an existence of multiple breaks in the observed, integrated along the line of sight, spectrum.

There is still a lot of work that has to be done to improve this model. Most importantly, the model should consider a spatial and energetic evolution of the nebula, a hadronic component and more complex injection spectrum as suggested by the current PIC simulations [85, 93].

4.4 References

[82] Begelman M., & Li Z.-Y., 1992, ApJ, 397, 187
[83] Chevalier R. A., 2000, ApJ, 539, L45
[84] de Jager O. C., et al., 2009, *arXiv:0906.2644*
[85] Fang J. & Zhang L., 2010, A&A, (*in press*), *arXiv:1003.1656v1*
[86] Gelfand J., et al., 2009, ApJ, 703, 2051
[87] Kennel C. F., Coroniti F. V., 1984, ApJ, 283, 71030
[88] Komissarov S. S. & Lyubarsky Y. E., 2003, MNRAS, 344, L93
[89] Pacini F., Salvati M., 1973, ApJ, 186, 24965
[90] Reynolds S. P., 2003, *In Cosmic Explosions: On the 10th Anniversary of SN 1993J (IAU Colloquium 192)*, astro-ph/0308483
[91] Reynolds S. P., 2009, ApJ, 703, 662
[92] Slane P., Chen Y., Schulz N. S., Seward F. D., Hughes J. P., Gaensler B. M., 2000, ApJ, 533, L2932
[93] Spitkovsky A., 2008, ApJ, 682, L5
[94] Volpi D., et al., 2008, A&A, 485, 337
[95] Willingale R., Aschenbach B., Griffiths R. G., Sembay S., Warwick R. S., et al., 2001, A&A, 365, L21217
[96] Woltjer L., Salvati M., Pacini F., Bandiera R., 1997, A&A, 325, 29599

A. Solving the kinetic equation

In spherical coordinates *div* and *grad* can be written through the normalized distance $z = r/r_0$ in a following way:

$$div = \frac{1}{r_0 z^2}\frac{\partial}{\partial z}z^2 \tag{A.1}$$

$$grad = \frac{1}{r_0}\frac{\partial}{\partial z} \tag{A.2}$$

Here all quantities have a simple power-law dependence on the normalized spatial coordinate z

$$B(z) = B_0 z^n \tag{A.3}$$

$$D(\gamma, z) = D_0 z^l \tag{A.4}$$

$$V(z) = V_0 z^m \tag{A.5}$$

$$b(\gamma, z) = b(\gamma) z^k \tag{A.6}$$

$$Q(\gamma_0, z) = \frac{K\gamma_0^{-\Gamma}}{4\pi z^2 r_0^2} \tag{A.7}$$

$b(\gamma, z)$ is an energy loss rate. $Q(\gamma_0, z)$ is a source function.

Therefore eq. 4.1 can be rewritten as

$$-\frac{D_0}{r_0^2 z^2}\frac{\partial}{\partial z}\left(z^{2+l}\frac{\partial N}{\partial z}\right) + \frac{V_0}{r_0 z^2}\frac{\partial}{\partial z}\left(z^{m+2}N\right) + z^k\frac{\partial}{\partial \gamma}\left(b(\gamma)N\right) = 0 \tag{A.8}$$

Lets define a new function $G(\gamma, z) = z^{m+2}b(\gamma)N(\gamma, z)$. After multiplying eq. A.8 by $z^2 r_0^2 \dfrac{b(\gamma)}{D_0}$ we get:

$$-\frac{\partial}{\partial z}\left(z^{2+l}\frac{\partial(z^{-m-2}G)}{\partial z}\right)+\frac{V_0 r_0}{D_0}\frac{\partial G}{\partial z}+z^{k-m}r_0^2\frac{b(\gamma)}{D_0}\frac{\partial G}{\partial \gamma}=0 \tag{A.9}$$

Lets define a new variable

$$\tau=\frac{D_0}{r_0^2}\int_{\gamma_0}^{\gamma}\frac{d\gamma}{b(\gamma)} \tag{A.10}$$

$$z^{l-m}\frac{\partial^2 G}{\partial z^2}+(l-2m-2)z^{l-m-1}\frac{\partial G}{\partial z}-(m+2)(l-m-1)z^{l-m-2}G \\ -\frac{V_0 r_0}{D_0}\frac{\partial G}{\partial z}-z^{k-m}\frac{\partial G}{\partial \tau}=0 \tag{A.11}$$

$$\frac{\partial^2 G}{\partial z^2}+(l-2m-2)z^{-1}\frac{\partial G}{\partial z}-(m+2)(l-m-1)z^{-2}G \\ -z^{m-l}\frac{V_0 r_0}{D_0}\frac{\partial G}{\partial z}-z^{k-l}\frac{\partial G}{\partial \tau}=0 \tag{A.12}$$

$$\frac{\partial^2 G}{\partial z^2}+\left((l-2m-2)z^{-1}-z^{m-l}\frac{V_0 r_0}{D_0}\right)\frac{\partial G}{\partial z} \\ -(m+2)(l-m-1)z^{-2}G-z^{k-l}\frac{\partial G}{\partial \tau}=0 \tag{A.13}$$

For the range for z, considered in this problem, we will have $\frac{V_0 r_0}{D_0}z^{m-l+1}\gg 1$

$$\frac{\partial^2 G}{\partial z^2}-\left(z^{m-l}\frac{V_0 r_0}{D_0}\right)\frac{\partial G}{\partial z}-(m+2)(l-m-1)z^{-2}G-z^{k-l}\frac{\partial G}{\partial \tau}=0 \tag{A.14}$$

We will look for a variable change $x=f(z)+g(\tau)\ ;\ y=\tau$ with the properties specified later.

$$\frac{\partial}{\partial z}=\frac{\partial f(z)}{\partial z}\frac{\partial}{\partial x} \\ \frac{\partial}{\partial \tau}=\frac{\partial g(\tau)}{\partial \tau}\frac{\partial}{\partial x}+\frac{\partial}{\partial y} \tag{A.15}$$

Hence eq. A.14 will have the following form

$$\left(\frac{\partial f(z)}{\partial z}\right)^2 \frac{\partial^2 G}{\partial x^2} - \left(z^{m-l}\frac{V_0 r_0}{D_0}\left(\frac{\partial f(z)}{\partial z}\right) + z^{k-l}\left(\frac{\partial g(\tau)}{\partial \tau}\right)\right)\frac{\partial G}{\partial x} - (m+2)(l-m-1)z^{-2}G - z^{k-l}\frac{\partial G}{\partial y} = 0 \tag{A.16}$$

We can choose the functions $f(z)$ and $g(\tau)$ in a following way:

$$f(z) = \begin{cases} \dfrac{z^{k-m+1} - z_0^{k-m+1}}{k-m+1}, & \text{if } k-m+1 \neq 0 \\ \ln\left(\dfrac{z}{z_0}\right), & \text{if } k-m+1 = 0 \end{cases} \tag{A.17}$$

$$g(\tau) = -\frac{V_0 r_0}{D_0}\,\tau \tag{A.18}$$

Then the differential equation for function G will have the form:

$$\left(\frac{\partial f(z)}{\partial z}\right)^2 \frac{\partial^2 G}{\partial x^2} - (m+2)(l-m-1)z^{-2}G - z^{k-l}\frac{\partial G}{\partial y} = 0 \tag{A.19}$$

$$z^{2k-2m}\frac{\partial^2 G}{\partial x^2} - (m+2)(l-m-1)z^{-2}G - z^{k-l}\frac{\partial G}{\partial y} = 0 \tag{A.20}$$

If $k-m+1 \neq 0$ then multiplying whole equation by z^2 and substituting $z^{k-m+1} = z_0^{k-m+1} + (k-m+1)\left(x + \dfrac{V_0 r_0}{D_0} y\right)$ in (A.20) gives

$$\left(z_0^{k-m+1} + (k-m+1)\left(x + \frac{V_0 r_0}{D_0} y\right)\right)^2 \frac{\partial^2 G}{\partial x^2} - (m+2)(l-m-1)G - \left(z_0^{k-m+1} + (k-m+1)\left(x + \frac{V_0 r_0}{D_0} y\right)\right)\frac{k-l+2}{k-m+1}\,\frac{\partial G}{\partial y} = 0 \tag{A.21}$$

If $k-m+1 = 0$ then substituting $\partial f/\partial z = z^{-1}$ in (A.19) gives

$$\frac{\partial^2 G}{\partial x^2} - (m+2)(l-m-1)G - z_0^{k-l+2}\exp\left((k-l+2)\left(x + \frac{V_0 r_0}{D_0} y\right)\right)\frac{\partial G}{\partial y} = 0 \tag{A.22}$$

A.1 Pulsar Wind Nebulae

In this section we consider two-zone model and adopt KC84 solutions for the radial dependence of the flow velocity and magnetic field. All the quantities are normalized with respect to their values at the flow transition distance from the PWN center - $r_0 = r_s(3\sigma)^{-1/2}$. With subscript "s" we denote the values of quantities at the termination shock.

$r_0 = r_s(3\sigma)^{-1/2}$
$V_0 = \sigma c$
$B_0 = B_s(3\sigma)^{-1/2}$

Then the flow speed and the magnetic field will exhibit following behavior in each zone:

Near zone : $(3\sigma)^{1/2} \leq z \leq 1$

$$V(z) = \frac{V_0}{z^2}$$
$$B(z) = B_0 z$$

Far zone : $1 \leq z \leq z_{PWN}$

$$V(z) = V_0$$
$$B(z) = \frac{B_0}{z}$$

We will determine the energy ranges for which adiabatic losses dominate over synchrotron and vise versa in the far zone (adiabatic loss rate equals to zero in the near zone).

$$b(\gamma, z)_{adiabatic} = \frac{\gamma \nabla V(z)}{3} = \frac{2\gamma V_0}{3 r_0 z} \tag{A.23}$$

$$b(\gamma, z)_{synchrotron} = \beta B(z)^2 \gamma^2 = \frac{\beta B_0^2 \gamma^2}{z^2} \tag{A.24}$$

So, if $\gamma \ll \dfrac{V_0}{\beta B_0^2 r_0} \equiv \gamma^\star$ then $\dfrac{b(\gamma, z)_{adiabatic}}{b(\gamma, z)_{synchrotron}} \gg 1$

and if $\gamma \gg \dfrac{V_0 z_{max}}{\beta B_0^2 r_0} = \gamma^\star z_{PWN}$ then $\dfrac{b(\gamma, z)_{adiabatic}}{b(\gamma, z)_{synchrotron}} \ll 1$

For $r_s \simeq 10^{16} cm$; $B_s \simeq 10^{-3} G \quad \Rightarrow \quad \gamma^\star \simeq 5 \cdot 10^8 \sigma^{5/2}$

A.1.1 Near Zone

In the Near zone

$$\begin{aligned} n &= 1 \\ m &= -2 \\ k &= 2 \\ l &= -1 \end{aligned} \tag{A.25}$$

$z_0 = z_s = (3\sigma)^{1/2}$. We will assume that $l = -1$. And since in the near zone we do not have the adiabatic losses, $k = 2$ for synchrotron losses ($b(\gamma, z) = \beta B(z)^2 \gamma^2$).

$(A.25) \Rightarrow \; k - m + 1 \neq 0$

Hence

$$(z_s^5 + 5\,(x + \xi y))^2 \frac{\partial^2 G}{\partial x^2} - (z_s^5 + 5\,(x + \xi y)) \frac{\partial G}{\partial y} = 0 \tag{A.26}$$

$$(z_s^5 + 5\,(x + \xi y))\frac{\partial^2 G}{\partial x^2} - \frac{\partial G}{\partial y} = 0 \tag{A.27}$$

Here

$$\xi = \frac{V_0 r_0}{D_0}$$

$$G(\gamma, z) = \beta B_0^2 \gamma^2 N(\gamma, z) \tag{A.28}$$

$$y = \frac{D_0}{\beta B_0^2 r_0^2}\left(\frac{1}{\gamma} - \frac{1}{\gamma_0}\right) \tag{A.29}$$

$$x = \frac{z^5 - z_s^5}{5} - \frac{V_0}{\beta B_0^2 r_0}\left(\frac{1}{\gamma} - \frac{1}{\gamma_0}\right) \tag{A.30}$$

and in terms of $\gamma^\star$

$$y = \frac{\gamma^\star}{\xi}\left(\frac{1}{\gamma} - \frac{1}{\gamma_0}\right) \tag{A.31}$$

$$x = \frac{z^5 - z_s^5}{5} - \gamma^\star\left(\frac{1}{\gamma} - \frac{1}{\gamma_0}\right) \tag{A.32}$$

Instead of (A.27) we will solve approximate equation. To get the approximate equation we will make some assumptions. i) For low energy electrons radiative decay is not important, therefore $\frac{1}{\gamma} - \frac{1}{\gamma_0} \ll 1$. ii) For high energy electrons

$$\frac{1}{\gamma} - \frac{1}{\gamma_0} \sim \frac{1}{\gamma} \tag{A.33}$$

and for high enough γ then $x \gg \xi y$ so

$$5x\frac{\partial^2 G}{\partial x^2} - \frac{\partial G}{\partial y} = 0 \tag{A.34}$$

We have to find the solution of (A.34) which equals to zero at the infinity and to the injection spectrum at the termination shock, $z = z_s$.

Such solution has the form

$$n_{Near}(\gamma, z) = \frac{(\Gamma - 1)K\gamma^{-\Gamma}}{4\pi r_0^2} \int_1^\infty d\epsilon \; \epsilon^{-\Gamma} exp\left[-\frac{\xi\gamma(z^5 - z_s^5)}{25\gamma^* \left(1 - \frac{1}{\epsilon}\right)} \right] \tag{A.35}$$

Here $\epsilon = \gamma_0/\gamma$. It could be seen from (A.35) that cut-off lorentz factor $\sim \frac{\gamma^*}{\xi}$

A.1.2 Far Zone

In the Far zone

$$n = -1$$
$$m = 0 \tag{A.36}$$

$$k = -1 \text{for adiabatic losses} (\gamma \ll \gamma^\star) \tag{A.37}$$

$$k = -2 \text{for synchrotron losses} (\gamma \gg \gamma^\star) \tag{A.38}$$

We will assume that $l = 1$, $z_0 = 1$

A.1.3 Far Zone: Low Energies

$(A.36)(A.37) \Rightarrow k - m + 1 = 0$

Hence

$$\frac{\partial^2 G}{\partial x^2} - \frac{\partial G}{\partial y} = 0 \tag{A.39}$$

Here

$$G(\gamma, z) = \frac{2V_0}{3r_0}\gamma z^2 N(\gamma, z) \tag{A.40}$$

$$y = \frac{3}{2\xi}\ln\left(\frac{\gamma_0}{\gamma}\right) \tag{A.41}$$

$$x = \ln(z) - \frac{3}{2}\ln\left(\frac{\gamma_0}{\gamma}\right) \tag{A.42}$$

Here, we have to match the solution of (A.39) with already obtained solution for the Near zone at the flow transition point $z = 1$, and with the solution of the kinetic equation without diffusion at the shock, $z = z_{PWN}$. Resulted electron density will be:

$$\begin{aligned} n_{Far}^{Low}(\gamma, z) &= \frac{C1(\gamma^*, \xi, \sigma, z_{PWN})}{z^2}\int_\gamma^\infty \frac{d\gamma_0\ n_{Near}(\gamma_0, 1)}{\left(\ln\left(\frac{\gamma_0}{\gamma}\right)\right)^{1/2}} \\ &\times \quad exp\left[-\frac{\xi\left(\ln z - \frac{3}{2}\ln\left(\frac{\gamma_0}{\gamma}\right)\right)^2}{6\ln\left(\frac{\gamma_0}{\gamma}\right)}\right] \end{aligned} \tag{A.43}$$

A.1.4 Far Zone: High Energies

$(A.36)(A.38) \Rightarrow k - m + 1 \neq 0$

Hence

$$(1 - (x + \xi y))^2\frac{\partial^2 G}{\partial x^2} - (1 - (x + \xi y))\frac{\partial G}{\partial y} = 0 \tag{A.44}$$

$$(1-(x+\xi y))\frac{\partial^2 G}{\partial x^2}-\frac{\partial G}{\partial y}=0 \tag{A.45}$$

Here

$$G(\gamma,z)=\beta B_0^2\gamma^2 z^2 N(\gamma,z) \tag{A.46}$$

$$y=\frac{D_0}{\beta B_0^2 r_0^2}\left(\frac{1}{\gamma}-\frac{1}{\gamma_0}\right) \tag{A.47}$$

$$x=\left(1-\frac{1}{z}\right)-\frac{V_0}{\beta B_0^2 r_0}\left(\frac{1}{\gamma}-\frac{1}{\gamma_0}\right) \tag{A.48}$$

and in terms of $\gamma^\star$

$$y=\frac{\gamma^\star}{\xi}\left(\frac{1}{\gamma}-\frac{1}{\gamma_0}\right) \tag{A.49}$$

$$x=\left(1-\frac{1}{z}\right)-\gamma^\star\left(\frac{1}{\gamma}-\frac{1}{\gamma_0}\right) \tag{A.50}$$

Here we approximate equation (A.45) as

$$\frac{\partial^2 G}{\partial x^2}-\frac{\partial G}{\partial y}=0 \tag{A.51}$$

It is reasonable to do so, since $\gamma \gg \gamma^\star$

Here, as well as in the previous case, we have to match the solution of (A.51) with already obtained solution for the Near zone at the flow transition point $z=1$, and to the solution of the kinetic equation without diffusion at the shock, $z=z_{PWN}$. As a result:

$$n_{Far}^{High}(\gamma, z) = \frac{C2(\gamma^*, \xi, \sigma, z_{PWN})}{z^2}\ \gamma^{-1/2} \int_{\gamma}^{\infty} \frac{d\gamma_0\ n_{Near}(\gamma_0, 1)}{\left(1 - \frac{\gamma}{\gamma_0}\right)^{1/2}}$$
$$\times\ exp\left[-\frac{\xi\gamma\left(1 - \frac{1}{z} - \gamma^*\left(\frac{1}{\gamma} - \frac{1}{\gamma_0}\right)\right)^2}{4\gamma^*\left(1 - \frac{\gamma}{\gamma_0}\right)} \right] \tag{A.52}$$

VITA

David Lomiashvili was born on November 1, 1982 in Tbilisi, Georgia (*the country*). He graduated *summa cum laude* from Tbilisi State University (TSU) with a B.S. in Computational Physics in 2003 and with a M.S. in Plasma Physics in 2005. After his M.S. studies, David co-founded a computer hardware company in Tbilisi and managed it for two years. When he came to Purdue University as a Ph.D. student, he undertook theoretical studies about various astrophysical phenomena and worked on number of projects, including explaining properties of radio emission from the double pulsar and solving particle transport equations in supernova remnants and pulsar wind nebulae.